01

Processing of thermoelectric converter data considering substrate material properties

© Yu.V. Dobrov, P.S. Eremenko, V.A. Lashkov

St. Petersburg State University,
199034 St. Petersburg, Russia
e-mail: y.dobrov@spbu.ru

Received November 15, 2023
Revised February 29, 2024
Accepted March 18, 2024

This paper introduces a comprehensive mathematical model for a gradient heat flux sensor, which accounts for substrate properties, and explores the influence of substrate parameters on sensor performance. Through a comparative analysis, we juxtapose this model with an alternative data processing approach that disregards substrate properties and assumes zero heat flux on the rear side. Our investigation exposes a substantial dependence of the collected data on the thermophysical attributes of the substrate. Additionally, experimental data acquired from the sensor, measuring heat flux density from a known source, undergo processing using the proposed model to assess its effectiveness.

Keywords: gradient heat flux sensor, thermometry, signal processing technique.

DOI: 10.61011/TP.2024.05.58514.286-23

Introduction

Most recently to measure heat fluxes sensors which operation principle is based on the transverse Seebeck effect [1], which is determined by the generation of EMF in an anisotropic medium in the direction perpendicular to the temperature gradient [2], are widely used.

Scheme of gradient heat flux sensor (GHFS) based on transverse Seebeck effect, is shown in Fig. 1. Thermoelement *1* with length l and thickness h is located on isolating mica substrate *2* attached to the studied surface. Via the work surface of the thermoelement the heat flux Q passes, due to it the temperature distribution is formed with temperatures on face T_h and back T_b sides of the thermoelement. As result on opposite sides of the thermoelement the electric voltage U appears.

If the thermoelement is sufficiently long, and temperature distribution is one-dimensional (at ratio $l/h > 10$ this assumption can be assumed as acceptable), then we can use Thomson formula, which sets the relationship of voltage generated by GHFS with difference of temperatures on back and face surfaces

$$U = \alpha_{xy}(T_h - T_b)\,\frac{l}{h}, \tag{1}$$

where U — voltage arising on the sensor, α_{xy} — component of thermo-emf tensor. Theory of thermal conductivity ensures link between the difference of temperatures on face and back surfaces of the thermoelement with density of heat flux, and thus according to the measured voltage on GHFS to restore the heat flux changing in time.

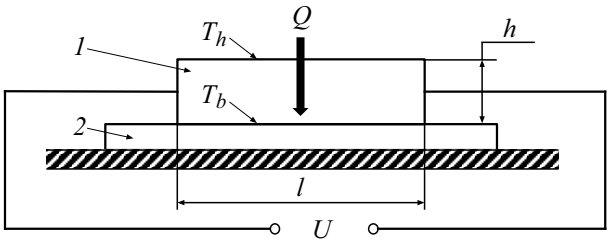

Figure 1. Schema of gradient heat flux sensor.

Such sensors attract by rather high spectrum of work temperatures and quick response [3]. Interest to the heat flux sensors is determined by the possibility of their use in different practical units [4,5].

Thin film sensors ALTP (atomic layer thermopile), manufactured using sputtering , are sensors with small time of reaching the stationary heat mode. Studies relating ALTP calibration show that sensors have low inertia and allow measurement of heat flux without additional signal processing [6,7,8]. In paper [9] we studied properties of sensor ALTP, which has time resolution at least 1 μs, and presents results of heat flux measurements in shock tube.

GHFSs are manufactured based on anisotropic thermoelements. Issue of GHFS applicability for study of quick changing heat fluxes is of interest, during their manufacturing the anisotropic single-crystals of high-purity bismuth are used [10]. Paper [11] states that in quick running gas dynamic processes with characteristic time over 20 ms GHFS based on bismuth can be used for direct measurement of heat flux. This sensor use at lower characteristic times (about 1 μs and below) is actual problem.

In present paper GHFS manufactured in Peter the Great Saint-Petersburg Polytechnic University is studied, in which

anisotropic bismuth single-crystal were used [10]. The sensor has small dimensions and comprises 10 thermoelements connected in series. Its face surface is a square with side $d = 2\,\text{mm}$. Transverse dimensions of thermoelement are $0.2 \times 0.2\,\text{mm}$. The sensor is installed on mica substrate. Gradient heat flux sensors (GHFS) can operate in a wide range of heat fluxes and temperatures. We think that development and updating of the method of sensor signal processing are important, the method ensures its use when measuring quick flowing heat fluxes.

If method of estimation of the time constant for the sensor to reach the steady state mode, presented in the work [9] is used:

$$\tau \approx 0,4\frac{\delta^2}{a},$$

where δ — sensor thickness, α — thermal diffusivity coefficient of the sensor material, then for the studied sensor based on bismuth we obtain the value about 2.5 ms, which by three orders of magnitude exceeds the time for sensor ALTP.

But papers [12,13] showed that the gradient sensor based on crystalline bismuth can be also used to measure heat fluxes, which characteristic time is below $1\,\mu$s. In this case for determination of high-speed pulsations of heat flux it is suggested to use special mathematical processing of the signal, which determines link between difference of temperatures on sensor sides and density of heat flux.

To determine the heat flux in quick running processes we need to solve the inverse problem: by change in difference of temperature on sensor the nature of behavior and value of heat flux are restored. For the inverse integral problem solution we need to make mathematical models of sensor which differ by various boundary conditions, for example, permanent temperature or absence of heat flux on back surface of the sensor. Such approaches neglect the fact that the sensor is installed on the substrate. For example, the suggested model of sensor [13] assumes that it is installed on the substrate with zero thermal activity (is an ideal thermal insulator), which is presented in form:

$$\varepsilon = \sqrt{c_p \rho_p \lambda_p},$$

where c_p, ρ_p, λ_p — respectively heat capacity, density and thermal conductivity coefficient of substrate material. But actual thermal insulating materials have non-zero thermal conductivity. So, during study of more prolonged processes (over 1 ms) we need to consider thermal interaction if sensor, substrate and, in general case, wall on which the sensor is installed. If the wall has high thermal activity then the problem can be simplify, leave only the sensor and the substrate, and assume that on the back side of the substrate the temperature does not change.

It is obvious that the thermal activity of the substrate will affect the nature of sensor useful signal, this was shown in paper [14]. The paper considered how the use of the substrate made of material with high thermal conductivity would affect the thermo-emf generated in the sensor. It is shown that when such substrate is used the temperature distribution in sensor stays close to the one-dimensional even under long-term action of heat flux (about several seconds), i.e. decreases uncertainty of the obtained data, and also increases value of generated thermo-emf.

In paper [15] the operation of thin film sensor is analyzed, several sensor models are discussed. When solving problem of thermal conductivity we consider the insulating substrate and metal base, on which the sensor is installed, but effect of the sensitive element (film) of sensor on the heat fluxes is assumed negligibly small. It is shown that the sensor can be used to measure density of heat fluxes during testing of the rotating turbines.

The present paper objective was making the mathematical model of the gradient heat flux sensor considering the thermophysical features of substrate, determination of analytical solution of thermal conductivity problem of to contacting plates and study of substrate parameters effect on sensor operation. Solution of the inverse problem: determination of heat flux density by temperature distribution and comparison of calculation results with experimental data. Show that GHFS based on bismuth using the suggested method can be used to measure quickly changing heat fluxes.

1. Field of temperature of two unlimited plates

Paper [13] suggests description of the heat exchange process of GHFS with external medium using equation of thermal conductivity for infinitely thin plate with boundary conditions of the second kind. It is assumed that there is no heat flux on the back side , and initially the temperature has uniform distribution.

We know the solution of the thermal conductivity problem of unlimited plate with thickness $2R$, which is heated from both sides similarly from the source with constant density of heat flux q_c [16]. In middle plane of the plate there no heat flux. This solution was used to describe the thermal conductivity of sensor which thickness was taken as R.

Equation characterizing the difference of dimensionless temperatures $\Delta\vartheta(\tau)$ of sensor sides looks like

$$\Delta\theta(\tau) = \theta(R,\tau) - \theta(0,\tau)$$

$$= \frac{1}{2} + \sum_{n=1}^{\infty}(-1)^{n+1}\frac{2}{\mu_n^2}(\cos\mu_n - 1)\exp(-\mu_n^2 Fo), \qquad (2)$$

where $\theta(x,\tau) = \frac{\lambda(T(x,\tau)-T_0)}{q_c R}$, $Fo = \frac{a\tau}{R^2}$ — Fourier number, $\mu_n = \pi n$ — characteristic numbers, T_0 — initial temperature of plate. This formula analysis shows that upon increase in heating time the difference of dimensionless temperatures increases to $\lim\limits_{Fo\to\infty}\Delta\theta(\tau) = 0.5$. If at $n = 1$ we assume that $\mu_n^2 Fo = 1$, then we can obtain evaluation of characteristic time for sensor reaching the steady state mode, which for the studied GHFS is about $630\,\mu$s.

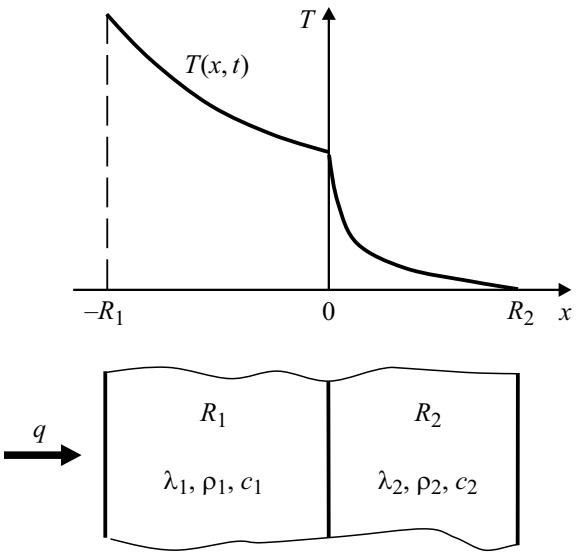

Figure 2. System of two unlimited plates.

During long-term effect of the heat flux the temperature increases not only on the face surface, but on back surface also. temperature of the back surface can be significant. But there is initial time interval when the temperature change of the back side of sensor can be neglected. This time corresponds to Fourier number $Fo \approx 0,1$ [16]. For studied GHFS this time is determined and is about ~ 0.6 ms. So, when studying the thermal processes which run quicker that this time period, we can consider the substrate effect on GHFS readings. GHFS heat transfer can be considered not taking into account the thermophysical properties of substrate material. Algorithm of sensor signal processing [13] was checked to measure the radiation heat flux from the laser spark and showed its ability to determine the high-speed thermal processes with characteristic time below $1\,\mu$s. Uncertainty of measurements by sensor of the heat flux density was about 7%. At more prolonged action of the heat flux there in need to consider the heat processes in substrate also. So, making of GHFS mathematical model considering these processes in substrate is actual.

Two unlimited plates with thickness R_1 and R_2 with different thermophysical coefficients are in contact (Fig. 2). The initial temperature of them is same, uniformly distributed and equal to T_0. To the face surface of system of plates the heat flux is supplied with constant density q, at the back surface constant temperature is maintained, equal to T_0. It is necessary ti find the temperature distribution in plate with thickness R_1 at time moment t.

Equation of thermal conductivity for the system of plates ($t > 0$):

$$\frac{\partial T_1(x,t)}{\partial t} = a_1 \frac{\partial^2 T_1(x,t)}{\partial x^2}, \quad -R_1 < x < 0,$$

$$\frac{\partial T_2(x,t)}{\partial t} = a_2 \frac{\partial^2 T_2(x,t)}{\partial x^2}, \quad 0 < x < R_2. \qquad (3)$$

Boundary conditions

$$T_1(x,0) = T_2(x,0) = T_0 = \text{const},$$

$$T_1(0,t) = T_2(0,t),$$

$$\frac{\lambda_1}{\lambda_2}\frac{\partial T_1(0,t)}{\partial x} = \frac{\partial T_2(0,t)}{\partial x},$$

$$\frac{\partial T_1(-R_1,t)}{\partial x} + \frac{q}{\lambda_1} = 0. \qquad (4)$$

Let's apply Laplace transform of partial differential equations with respect to a variable t and obtain common heterogeneous differential equation of second order with constant coefficients relative to image:

$$a_i \frac{d^2 T_L^{(i)}(x,s)}{dx^2} - s T_L^{(i)}(x,s) + u(x) = 0,$$

where function $u(x) = T_0 = \text{const}$ describes the initial distribution of temperature, i — plate number, a_i — thermal diffusivity of the plate. Using method of method of variation of arbitrary constants we can obtain solution having view:

$$T_L^{(i)}(x,s) = \frac{T_0}{s} + A_i(s)\,\mathrm{ch}\sqrt{\frac{s}{a_i}}x + B_i(s)\,\mathrm{sh}\sqrt{\frac{s}{a_i}}x.$$

Boundary conditions:

1) $T_2(R_2,t) = T_0 \to T_L^{(2)}(R_2,s) = \frac{T_0}{s}$,

2) $T_1(0,t) = T_2(0,t) \to T_L^{(1)}(0,s) = T_L^{(2)}(0,s)$,

3) $\frac{\lambda_1}{\lambda_2}\cdot\frac{\partial T_1(0,t)}{\partial x} = \frac{\partial T_2(0,t)}{\partial x} \to K_\lambda \frac{\partial T_L^{(1)}(0,s)}{\partial x} = \frac{\partial T_L^{(2)}(0,s)}{\partial x}$,

4) $\frac{T_1(-R_1,t)}{\partial x} + \frac{q(t)}{\lambda_1} = 0 \to \frac{\partial T_L^{(1)}(-R_1,s)}{\partial x} = -\frac{q}{\lambda_1 s}$, where $K_\lambda = \frac{\lambda_1}{\lambda_2}$. The problem was reduced to finding the coefficients $A_i(s)$ and $B_i(s)$, using boundary conditions 1−4. After substitution of found expressions for coefficients into equation (1) and solution equation relative to $T_L^{(1)}(x,s)$, we obtain image for temperature distribution on the face plate:

$$T_L^{(1)}(x,s) - \frac{T_0}{s} = -\frac{q}{\lambda_1}$$

$$\times \frac{\left(K_a^{\frac{1}{2}}\mathrm{ch}\sqrt{\frac{s}{a_2}}R_2\mathrm{sh}\sqrt{\frac{s}{a_1}}x - K_\lambda \mathrm{sh}\sqrt{\frac{s}{a_2}}R_2\mathrm{ch}\sqrt{\frac{s}{a_1}}x\right)}{s\sqrt{\frac{s}{a_1}}\left[K_\lambda \mathrm{sh}\sqrt{\frac{s}{a_2}}R_2\mathrm{sh}\sqrt{\frac{s}{a_1}}R_1 + K_a^{\frac{1}{2}}\mathrm{ch}\sqrt{\frac{s}{a_1}}R_1\mathrm{ch}\sqrt{\frac{s}{a_2}}R_2\right]}.$$

Use decomposition theorem. If $f_L(s) = \frac{\varphi(s)}{\psi(s)} = \frac{A_0 + A_1 s + A_2 s^2 + \cdots}{B_1 s + B_2 s^2 + \cdots}$, then $f(y) = L^{-1}[f_L(s)] = \sum\limits_{n=1}^{\infty} \frac{\varphi(s_n)}{\psi'(s_n)} e^{s_n y}$, where s_n — simple poles $\psi(s)$. Introducing designations $i\sqrt{\frac{s}{a_1}}R_1 = \mu$, $K_{R_2} = \frac{R_2}{R_1}$ and replacing $\mathrm{ch}z = \cos(iz)$, $\mathrm{sh}\,z = \frac{1}{i}\sin(iz)$ we obtain the characteristic equation

$$K_\lambda \,\mathrm{tg}\,\mu\,\mathrm{tg}\left(K_a^{\frac{1}{2}} K_{R_2}\mu\right) = K_a^{\frac{1}{2}}, \qquad (5)$$

where $K_a = \frac{a_1}{a_2}$.

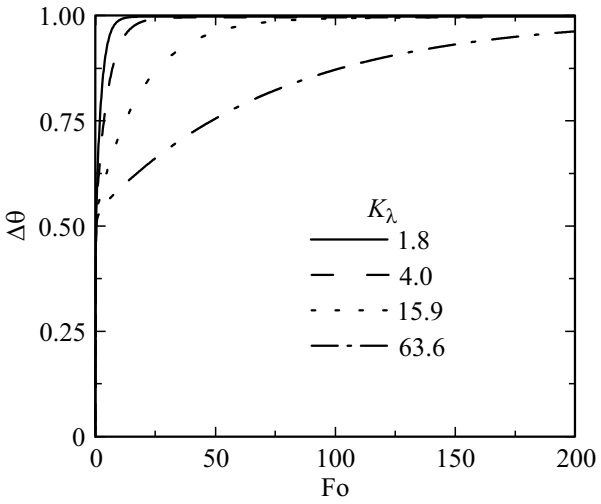

Figure 3. Dimensionless temperature difference of plate 1 vs. Fourier number and parameter K_λ

Making reverse Laplace transform we obtain original $T_L^{(1)}(x, s)$:

$$T_1(x,t) = T_0 - \frac{q}{\lambda_1}(x - K_\lambda R_2) + \frac{2R_1 q}{\lambda_1} \times \sum_{n=1}^{\infty} \frac{\left(K_a^{\frac{1}{2}} \cos\left(K_{R_2} K_a^{\frac{1}{2}} \mu_n\right) \sin\left(\frac{\mu_n x}{R_1}\right) - \right.}{\mu_n^2 [K_a^{\frac{1}{2}} (K_\lambda K_{R_2} + 1)] \cos(K_{R_2} K_a^{\frac{1}{2}} \mu_n) \sin\mu_n + \left. -K_\lambda \sin\left(K_{R_2} K_a^{\frac{1}{2}} \mu_n\right) \cos\left(\frac{\mu_n x}{R_1}\right)\right)} e^{-\frac{\mu_n^2 a_1 t}{R_1^2}} \cdot \\ + (K_\lambda + K_{R_2} K_a) \sin(K_{R_2} K_a^{\frac{1}{2}} \mu_n) \cos\mu_n \quad (6)$$

Let's find difference of dimensionless temperatures on sides of plate 1, which, obviously characterizes GHFS signal

$$\Delta\theta(t) = \frac{[T_1(-R_1, t) - T_1(0, t)]\lambda_1}{qR_1}. \quad (7)$$

Let's study what effect the thermophysical parameters of plate 2 (sensor substrate) have on difference of dimensionless temperatures provided that density of heat flux q is constant. The problem was solved at the following parameters: material of plate 1 — bismuth (density 9870 kg/m^3, heat capacity 126 J/(kg·K), thermal conductivity 7.95 W/(m·K), thickness 0.2 mm), material of plate 2 — mica (density 290 kg/m^3, heat capacity 880 J/(kg·K), thermal conductivity 0.5 W/(m·K). Thickness of plate 2 $R_2 = 0.2205$ mm was selected such that product $K_a^{\frac{1}{2}} K_{R_2}$ was integer. Such approach, not decreasing the generality of the results, ensures significant decrease in labor intensity of roots calculation of characteristic equation.

Fig. 3 presents results of calculation of dimensionless temperature difference $\Delta\theta$ on sides of plate 1 at $K_{R_2} = 1.1$.

With Fourier number increasing to $Fo = \frac{a_1 t}{R_1^2} = 0.2$ the temperature difference increases quickly to ~ 0.55 and practically does not depend on parameter K_λ. With further Fourier number increasing the increasing rate becomes significantly dependent on parameter K_λ. The higher it is, the slower increasing is. So, the lower the thermal conductivity of plate 2 (of sensor substrate) is, the slower sensor readings reach the constant value. The time it takes for temperature difference to reach the constant level can be rather large.

Fig. 4, *a* shows effect of parameter K_{R_2} on behavior of dimensionless temperature difference $\Delta\theta$ at $K_\lambda = 15.9$.

Character of behavior $\Delta\theta$ practically does not repeat. With *Fo* increasing to 0.2 the temperature difference quickly increase, with further increase in Fourier number the increasing rate $\Delta\theta$ depends on parameter K_{R_2}. The higher it is (the higher thickness of plate 2 is), the slower the temperature difference reaches the constant value. Fig. 4, *a* in another scale shows dependence $\Delta\theta$ at small values of Fourier number. At Fourier numbers below 0.2 the character of the dependence $\Delta\theta$ practically does not depend on parameters K_{R_2} and K_λ: all curves coincide.

Fig. 4, *b* presents dimensionless temperature difference determined by different models. Solid line — temperature difference calculated by formula (2), when it was accepted that heat flux on the back side of plate is equal to zero . The dashed line — temperature difference $\Delta\theta$ determined by formula (7), when we consider double plate, on back side of which wall temperature is registered. The case is presented when $K_{R_2} = 0.55$, $K_\lambda = 15.9$. Up to Fourier number 0.15–0.2 the lines coincide, at further *Fo* increasing the solid line reaches constant level 0.5, and dashed line continues rise to 1.

Let's present solution of thermal conductivity problem with heat flux non-constant over time on the face surface of the plates [16]. When determining time dependence of heat flux density on face surface of plate we assume that $q(t)$ corresponds to all requirements for image existence and has first derivative. Then using Duhamel integral we obtain the solution of the inverse problem and formula linking the temperature difference on sides of first plate with heat flux density

$$\Delta T_1(x,t) = \frac{2a_1}{\lambda_1 R_1} \int_0^t q(\tau) \times \sum \frac{\left(K_a^{\frac{1}{2}} \cos\left(K_{R_2} K_a^{\frac{1}{2}} \mu_n\right) \sin\left(\frac{\mu_n x}{R_1}\right) - \right.}{\left[K_a^{\frac{1}{2}} K_\lambda K_{R_2} + 1\right] \cos\left(K_{R_2} K_a^{\frac{1}{2}} \mu_n\right) \sin\mu_n + \left. -K_\lambda \sin\left(K_{R_2} K_a^{\frac{1}{2}} \mu_n\right)\left(\cos\left(\frac{\mu_n x}{R_1}\right) - 1\right)\right)} e^{-\frac{\mu_n^2 a_1 (t-\tau)}{R_1^2}} d\tau. \\ + (K_\lambda + K_{R_2} K_a) \sin\left(K_{R_2} K_a^{\frac{1}{2}} \mu_n\right) \cos\mu_n$$

This equation solution together with formula (1) ensures to determine link between EMF generated by sensor, and variable heat flux density. The inverse integral problem was solved by numerical method,the integral was presented using trapezoids.

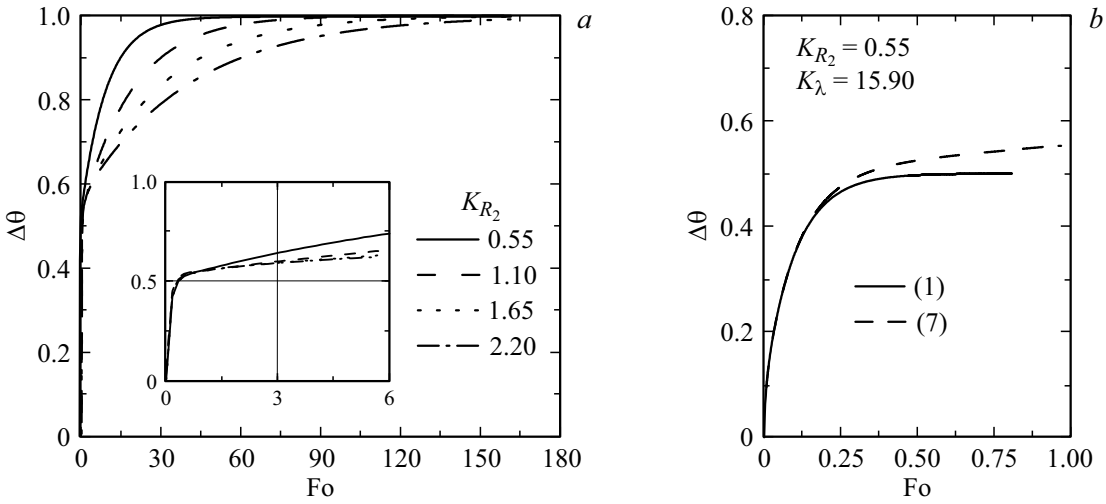

Figure 4. Dimensionless temperature difference of plate 1 vs. Fourier number and parameter K_{R_2}

2. Heat flux determination using GHFS based on bismuth

Sensor operation was studied at test stand described in [13]. As the radiation source we used halogen lamp 500 W. Radiation heat flux supplied from the source to sensor was formed using modulator. Two types of modulators were used: one of them was solid disk with holes rotating with constant speed (hereinafter referred to as fast modulator), second one — a metal curtain moved by an electromagnet (hereinafter referred to as a slow modulator). The first modulator permits GHFS opening for time in range 1−4 ms, second one —for 300−600 ms. Using photodiode FD-24K the supply of radiation flow on GHFS was monitored. Radiation power was registered by average power meter IMO-2. In place of sensor installation the optical system created uniform heat flux with density $q_L = 4.16\,\text{kW/m}^2$. Considering reflective ability of bismuth (emissivity coefficient of bismuth $\varepsilon \approx 0.34$ [17]) the GHFS surface was exposed to heat flux with density $q = \varepsilon q_L = 1.41\,\text{kW/m}^2$. To perform thorough calibration of the sensor, we should known, of cause, the value of emissivity coefficient with high reliability. This is separate solved problem [18]. Our study objective is to show that using the developed method of the sensor signal processing we can restore the time characteristics of heat flux varying over time. The sensor signal after amplifier (gain $K_{am} = 175$, bandwidth to 10 MHz) entered the oscilloscope Tektronix TDS2022.

Fig. 5, *a* presents the photodiode signal, and in Fig. 5, *b* — GHFS data during operation with slow modulator, in Fig. 5, *c* — results of inversion problem solution. The photodiode signal shows that on GHFS the heat flux of constant level is supplied, and time of sensor opening process is about 2 ms, time when sensor is in completely open state is 330 ms. When heat flux appears on GHFS voltage from its output initially quickly increase, then rather slowly for 200 ms reaches the constant value $U_m = 13.5\,\text{mV}$. In our case Fourier number $Fo = 1$ corresponds to 6 ms, then GHFS signal reaches constant maximum value at $Fo = 35$. The parameter $K_{R_2} = 0.55$ corresponds to such time of constant level reaching (Fig. 4, *a*), i.e. thickness of sensor substrate corresponds to 0.1 mm. So when solving the inverse problem of thermal conductivity this parameter is assumed as actual one.

Fig. 5, *c* present the result of calculation of heat flux density as per GHFS readings (gray line), black line — calculation results smoothening using Fourier method. The heat flux density reaches the level $q_c = 1.23\,\text{kW/m}^2$, which stays constant for all time when GHFS is open. It is obvious that to ensure matching of calculated heat flux density and the experimental density wee need to introduce correction calibration coefficient $K = \frac{q}{q_c} = 1.15$. Duration of calculated front of the heat flux corresponds to front of registered by the photodiode, i.e. it is about 2 ms. Results of method use [13] showed that in this case the calculated density of heat flux does not reach the constant level, which does not correspond the experimental conditions, and monotonic. although small, increase is observed.

Fig. 6 shows results of GHFS study on fast modulator.

Time of sensor opening at level 0.5 corresponds to 810 μs. Opening front — 420 μs (Fig. 6, *a*). Time characteristics of calculated heat flux density (Fig. 6, *c*) and signal from photodiode (Fig. 6, *a*) are in good agreement. Amplitude of GHFS signal was about 5 mV (Fig. 6, *b*), calculated heat flux density reached $1.18\,\text{kW/m}^2$ (Fig. 6, *c*). Black line — results of solution data filtering using Fourier method. Results of heat flux density calculation using two methods (suggested in present paper and method from paper [13]) coincide.

Fig. 7 presents results of heat flux measurements, when time of sensor opening corresponds to 4.2 ms (Fig. 7, *a*). Sensor was also closed using fast modulator. Time of sensor opening front — 420 μs. At that amplitude of GHFS signal

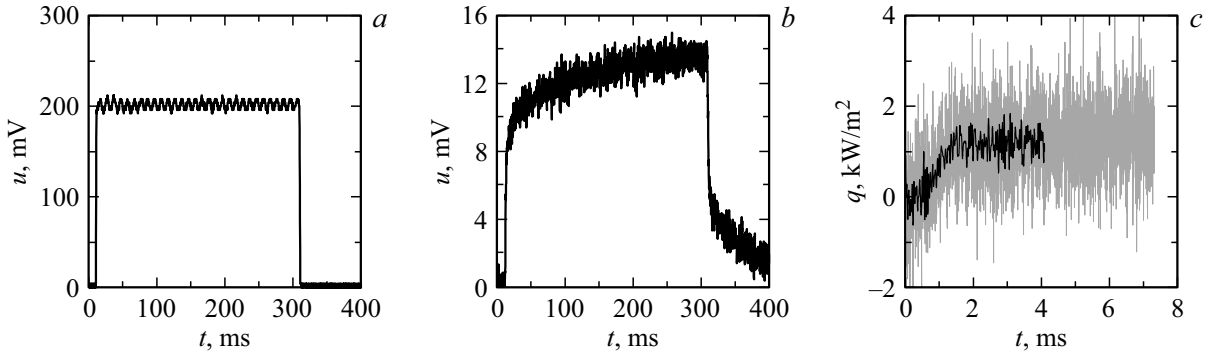

Figure 5. Characteristic measurements using slow modulator: *a* — photodiode readings, *b* — GHFS signal, *c* — heat flux density.

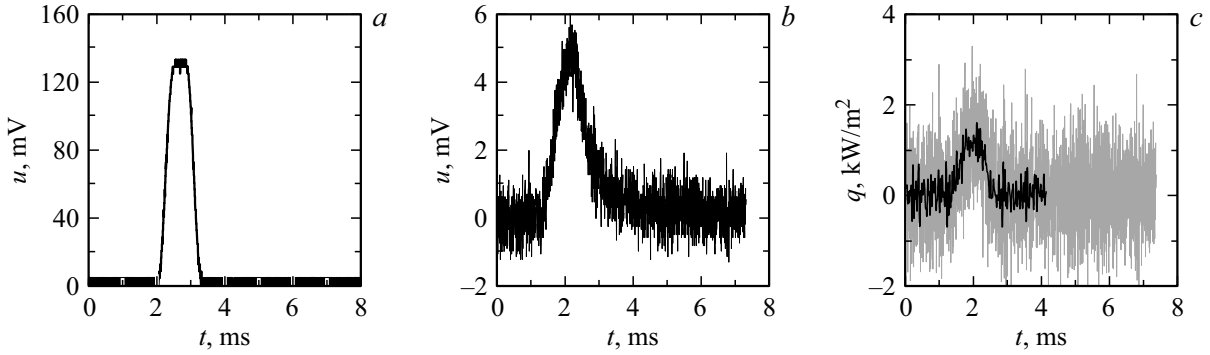

Figure 6. Characteristic measurements using fast modulator: *a* — photodiode readings, *b* — GHFS signal, *c* — heat flux density.

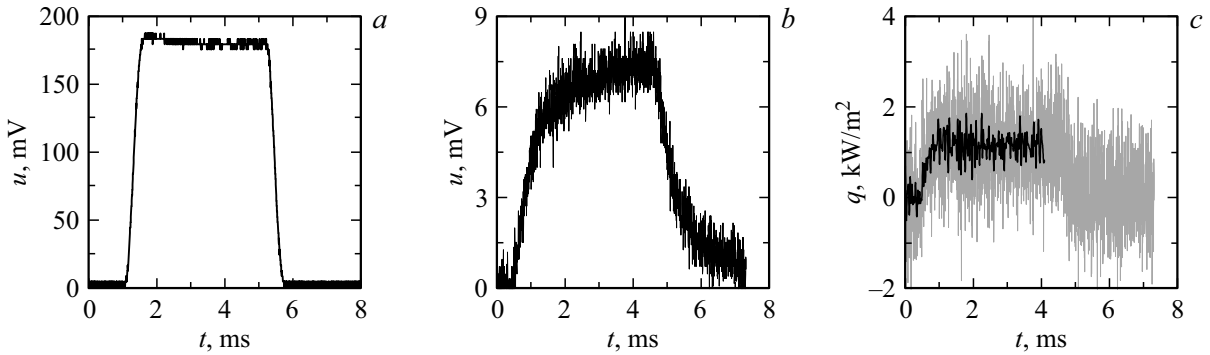

Figure 7. Characteristic measurements using fast modulator: *a* — photodiode readings, *b* — GHFS signal, *c* — heat flux density.

reached 7 mV (Fig. 7, *b*). When solving inverse problem of heat flux density determination oscillations occur (Fig. 7, *c*, gray line). In same Fig. 7, c the results of solution data filtering using Fourier method is shown (black line).

Black line initially shows the monotonic increase in heat flux density, which occurs as a result of sensor gradual opening by the modulator. This is confirmed by photodiode readings (Fig. 7, *a*). Then the heat flux density reaches constant level corresponding to about 1.23 kW/m^2.

Thus, using GHFS we measured the monitored heat flux density in rather wide range of sensor opening time: 0.8 to 330 ms. In full studied time range, which exceeds the time necessary for sensor signal to reach the constant level, the results of heat flux density calculation well coincide. The developed method of the sensor signal processing can be suggested to restore the heat flux measured using GHFS. GHFS based on bismuth can be successfully used when studying quick-changing thermal processes. The measured volt-watt coefficient of the studied device (GHFS+amplifier) is $S = \frac{U_m}{qd^2} = 2.39$ V/W, of GHFS itself — $S_s = \frac{S}{K_{am}} = 13.7$ mV/W.

Conclusions

New model of GHFS was suggested considering the thermophysical properties of substrate, on which the sensor is

installed. The mathematical model of two-layer infinite plate is studied, on back side of substrate the wall temperature was fixed.

The presented model was compared with another one, in which only one plate was considered, on its back side the heat flux present. temperature difference on sensor surfaces was compared at constant heat flux, the difference was determined by two said models. The analysis results show that time dependence of dimensionless temperature difference depends on thermophysical parameters and thickness of substrate.

We can distinguish three operation modes of the heat flux sensor:

1) pulse — characteristic time of process is below 1 ms, when effect of substrate on sensor readings can be neglected. Under these conditions the model of single plate with zero heat flux on back side can also operate;

2) transient — in discussed option $1-200$ ms (Fourier numbers $Fo = 0.5-35$), when effect of substrate om sensor readings shall be considered;

3) steady state — characteristic times of the thermal process are over 200 ms ($Fo > 35$). In this case the sensor manage to follow changes in heat flux, and there is no need to solve the inverse problem of thermal conductivity.

GHFS operation was studied. The suggested method of GHFS signal processing and calculation of heat flux density affecting the sensor well restored its time characteristics.

Funding

This study was financially supported by the Russian Science Foundation (project № 23-19-00241).

Conflict of interest

The authors declare that they have no conflict of interest.

References

[1] A.M. Kharitonov. *Tekhnika i metody aerofizicheskogo eksperimenta. Ch. 2. Metody i sredstva aerofizicheskikh izmerenij:* ucgebnik (Izd-vo HGTU, Novosibirsk, 2007), 455 c. (in Russian)

[2] A.G. Samoylovich. *Termoelektricheskie i termomagnitnye metody prevrashcheniya energii* (Izdatel'stvo LKI, M., 2007), 224 s. (in Russian)

[3] S.V. Bobashev, Yu.P. Golovachev, N.P. Mende, P.A. Popov, B.I. Reznikov, V.A. Sakharov, A.A. Schmidt, A.S. Chernyshev, S.Z. Sapozhnikov, V.Yu. Mityakov, A.V. Mityakov. ZhTF, **78** (12), 103 (2008). (in Russian).

[4] O.M. Alifanov, S.A. Budnik, A.V. Morzhukhina, A.V. Nenarokomov, A.V. Netelev, D.M. Titov. J. Engineeri. Phys. Thermophys., **91**, 26 (2018). DOI: 10.1007/s10891-018-1716-0

[5] P. Kennedy, J. Donbar, J. Trelewicz, Ch. Gouldstone, J. Longtin. 17th AIAA Intern. Space Planes and Hypersonic Systems and Technol. Conf., (11-14 April 2011, San Francisco, California), DOI: 10.2514/6.2011-2330

[6] T. Roediger, H. Knauss, U. Gaisbauer, E. Kraemer, S. Jenkins, J. von Wolfersdorf. J. Turbomach., **130** (1), 011018 (2008). https://doi.org/10.1115/1.2751141

[7] M. Collins, K. Chana, T. Povey. Meas. Sci. Technol., **26** (2), 025303 (2015). DOI: 10.1088/0957-0233/26/2/025303

[8] Zh. Liu, S. Liu, J. Zhao, Ya. Yue, Q. Xu, F. Yang. Measurement, **198**, 111419 (2022). DOI.org/10.1016/j.measurement.2022.111419

[9] H. Knauss, T. Roediger, D.A. Bountin, B.V. Smorodsky, A.A. Maslov, J. Srulijes. J. Spacecraft and Rockets, **46** (2), 255 (2009).

[10] S.Z. Sapozhnikov, V.YU. Mityakov, A.V. Mityakov. *Gradientnye datchiki teplovogo potoka* (Izd-vo SPbGPU, SPb., 2003), 168 s. (in Russian)

[11] S.V. Bobashev, N.P. Mende, P.A. Popov, B.I. Reznikov, V.A. Sakharov, S.Z. Sapozhnikov, V.Yu. Mityakov, A.V. Mityakov, D.A. Buntin, A.A. Maslov, H. Knauss, T. Rediger. Pis'ma v ZhTF, **35** (5), 36 (2009). (in Russian)

[12] P.A. Popov, S.V. Bobashev, B.I. Reznikov, V.A. Sakharov. Tech. Phys. Lett., **44** (4), 316 (2018).

[13] Yu.V. Dobrov, V.A. Lashkov, I.Ch. Mashek, A.V. Mityakov, V.Yu. Mityakov, S.Z. Sapozhnikov, R.S. Khoronzhuk. ZhTF, **91** (2), 240 (2021). (in Russian). DOI: 10.21883/JTF.2021.02.50357.209-20

[14] P.A. Popov, S.V. Bobashev, B.I. Reznikov, V.A. Sakharov. Pis'ma v ZhTF **43**, 7, (2017) (in Russian).

[15] J.E. Doorly, M.L.G. Oldfield. Intern. J. Heat and Mass Transfer, **30** (6), 1159 (1987). DOI: 10.1016/0017-9310(87)90045-7

[16] A.V. Lykov. *Teoriya teploprovodnosti* (Vysshaya Shkola, M., 1967), 600 s. (in Russian)

[17] *Naucho-tekhnicheskij tsentr „Ekspert" (nerazrushayuschij kontrol'), Koeffitsient izlucheniya (stepen' chernoty) razlichnykh materialov.* (in Russian) https://ntcexpert.ru/cg/57-acenter/teplovoj-kontrol/797-kojefficient-izluchenija-razlichnyh-materialov

[18] *Metrologiya teplofizicheskogo eksperimenta*, pod red. prof. S.Z. Sapozhkova (Izd-vo Politekhnicheskogo un-ta, SPb., 2017) (in Russian)

Translated by I.Mazurov